Analysis on the performance of reconfigurable intelligent surface-aided free-space optical link under atmospheric turbulence and pointing errors

Duong Huu Ai[1], Dai Tho Dang[2], Nguyen Vu Anh Quang[1], Van Loi Nguyen[2]
[1]Faculty of Computer Engineering and Electronics, Vietnam-Korea University of Information and Communication Technology, The University of Danang, Danang, Vietnam
[2]Faculty of Computer Science, Vietnam-Korea University of Information and Communication Technology, The University of Danang, Danang, Vietnam

Article Info

ABSTRACT

Free-space optical (FSO) communication can provide the cost-efficient, secure, high data-rate communication links required for applications. For example, it provides broadband internet access and backhauling for the fifth-generation (5G) and the sixth-generation (6G) communication networks. However, previous solutions to deal with signal loss caused by obstructions and atmospheric turbulence. In these solutions, reconfigurable intelligent surfaces (RISs) are considered hardware technology to improve the performance of optical wireless communication systems. This study investigates the pointing error effects for RIS-aided FSO links under atmospheric turbulence channels. We analyze the performance of RIS-aided FSO links influenced by pointing errors, atmospheric attenuation, and turbulence for the subcarrier quadrature amplitude modulation (SC-QAM) technique. Atmospheric turbulence is modeled using log-normal distribution for weak atmospheric turbulence. Several numerical outcomes obtained for different transmitter beam waist radius and pointing error displacement standard deviation are shown to quantitatively illustrate the average symbol error rate (ASER).

Corresponding Author:

Duong Huu Ai
Vietnam-Korea University of Information and Communication Technology, The University of Danang
Danang, Vietnam
Email: dhai@vku.udn.vn

1. INTRODUCTION

Free-space optical (FSO) communication is considered a nominee to help the high-speed connection necessities of 5G [1]. FSO systems are encouraged by their benefits compared to their radio frequency (RF) counterparts. The benefits of FSO systems are higher channel capacity, larger bandwidth, cost-effectiveness, unlicensed spectrum, and highly secured. Besides, both system design and setup are also uncomplicated [1]–[5]. Nevertheless, there are challenges when FSO transmits through the atmosphere, such as signal fading, attenuation, pointing errors, and signal obstruction [2]. We endeavor to crack the obstruction situation for FSO systems influenced by weak turbulence without pointing errors utilizing reconfigurable intelligent surfaces (RISs). RIS are electromagnetic devices with electronically controllable characteristics. They are able to refract, reflect, extinct, phase, and polarity.

Nowadays, using optical relay nodes is one useful resolution to solve the obstruction problem. The relay nodes are not cheap because of additional hardware deployment. RIS has proved their efficiency in

performance improvement for non-line-of-sight wireless systems. The RIS module is a planar array of multiple mirrors used to guide the incoming signal toward a targeted area and reconfigure the transmission channel [6]–[15]. It benefits wireless networks over other technologies, such as relay systems. Besides, RIS saves power and is made of electronically controllable elements. The benefits attract the interest of scientists [16]–[26].

Therefore, this study suggests a method for the execution of pointing error effects for RIS-aided FSO links under atmospheric turbulence. We theoretically analyzed the average symbol error rate signal-to-noise ratio (SNR) of RIS-assisted FSO links over log-normal turbulence channels. The paper's rest is organized as follows. Section 2 describes the system descriptions and channel model. Section 3 presents the average symbol error rate (ASER). Section 4 presents results and discussions. We conclude the study in section 5.

2.   SYSTEM AND CHANNEL MODELS
2.1. System model

Figure 1 presents our study problem. S is the signal source node, and D is the destination node. The signal from S is reflected on a RIS, then goes to D. Node S does not link directly to node D due to obstructions. The RIS module is placed at a suitable place and acts as a reflector. There are no obstructions that block transmitted light to the receiver. Assuming that the transmitted and reflected channels exhibit weak turbulence, the light passion over them undergoes the same attenuation grade. Besides, assuming that there is no pointing error.
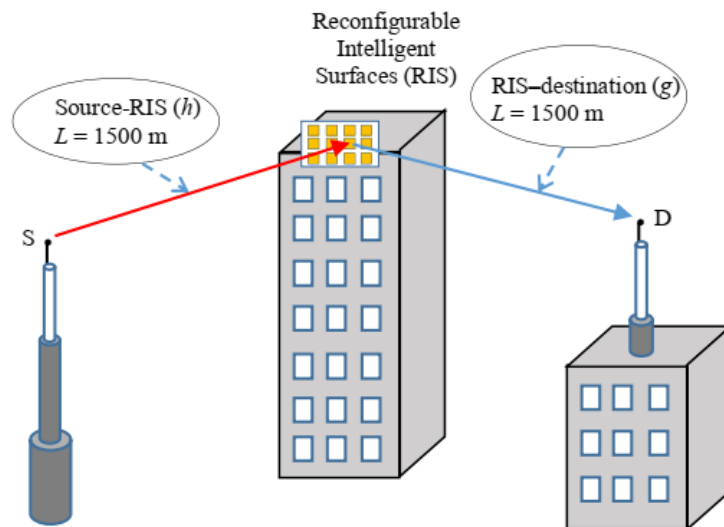

Figure 1. A model of RIS-aided FSO system

This study considers the factors characterizing an FSO channel. It comprises link loss, and pointing errors, atmospheric turbulence. Three major signal impairment elements of the FSO link are atmospheric turbulence (h_a), pointing errors (h_p), and attenuation (h_l).

$$h = h_l \times h_a \times h_p \qquad (1)$$

Atmosphere-induced turbulence is described by distribution models. In their study, Ai *et al.* [18] introduced the probability density function (pdf) of the irradiance intensity in the weak turbulent. For the weak turbulence, it is considered h_a as a spontaneous process with a log-normal distribution.

$$f_{h_a}(h_a) = \frac{1}{h_a \sigma_S \sqrt{2\pi}} exp\left(-\frac{[ln(h_a)+0.5\sigma_S^2]^2}{2\sigma_S^2}\right) \qquad (2)$$

where σ_S is the scintillation index, and is defined at [15] as $\sigma_S = exp(\omega_1 + \omega_2) + 1$; where

$$\omega_1 = \frac{0.49\sigma_2^2}{(1+0.18d^2+0.56\sigma_2^{12/5})^{7/6}} \tag{3}$$

$$\omega_2 = \frac{0.51\sigma_2^2(1+0.69\sigma_2^{12/5})^{-5/6}}{1+0.9d^2+0.62d^2\sigma_2^{12/5}} \tag{4}$$

In these equations, $d = \sqrt{kD^2/4L}$ where $k = 2\pi/\lambda$ is the optical wave number, λ is the wavelength, L is the link distance, and D is the radius of a circular receiving aperture, and σ_2 is the Rytov variance, and assuming spherical wave propagation. The Rytov is defined as, $\sigma_2^2 = 0.492C_n^2k^{7/6}L^{11/6}$ where C_n^2 is the refractive-index structure parameter, which is weather depended. The atmospheric attenuation is given by (5):

$$h_l = exp(-\sigma_l L_a) \tag{5}$$

where σ_l is the attenuation coefficient.

The propagation distance L_a is the link distance. The attenuation coefficient σ_l with the value of $\sigma_l(dB)$ [dB/km] is given by (6):

$$\sigma_l = \frac{3.91}{V[km]}\left(\frac{\lambda[nm]}{550}\right)^{-q} \tag{6}$$

where V is the visibility and q is the scattering particles' size distribution. q is computed by using Kim model, i.e.,

$$q = \begin{cases} 1.6 & V > 50 \\ 1.3 & 6 < V < 50 \\ 0.16V + 0.34 & 1 < V < 6 \\ V - 0.5 & 0.5 < V < 1 \\ 0 & V < 0.5 \end{cases} \tag{7}$$

The value of V is according to weather conditions. In [15], the PDF of X_p is shown as (8).

$$f_{h_p}(h_p) = \frac{\xi^2}{A_0^{\xi^2}} h_p^{\xi^2-1}, \qquad 0 \leq h_p \leq A_0 \tag{8}$$

In which $A_0 = [erf(v)]^2$: collected power's fraction at radial distance 0, $v = \sqrt{\pi}r/(\sqrt{2}\omega_z)$, r: aperture radius at the distance z, ω_z beam waist at the distance z. Equivalent beam radius is calculated by [15]:

$$\omega_{zeq} = \omega_z(\sqrt{\pi}\,erf(v)/2v \times exp(-v^2))^{1/2} \tag{9}$$

where $\omega_z = \omega_0[1 + \varepsilon(\lambda L/\pi\omega_0^2)^2]^{1/2}$ with ω_0 is the transmitter beam waist radius at $z = 0$, $\varepsilon = (1 + 2\omega_0^2)/\rho_0^2$ and $\rho_0 = (0.55C_n^2k^2L)^{-3/5}$ is the coherence length.

2.2. End-to-end signal-to-noise ratio

In this section, we assume that the RIS module has a reflective function without light through. Besides, assume the channel phases' perfect knowledge at RIS and destination. The detected signal is expressed as (10).

$$y = \sqrt{E_s}(hme^{jq}g)x + n \tag{10}$$

Where E_s is the symbol energy, h and g are respectively the S-RIS and RIS-D complex channel vectors [14], [19].

$$\gamma = \bar{\gamma}\left|h\mu e^{j\theta}g\right|^2 \tag{11}$$

Where $\bar{\gamma} = \frac{E_s}{N_0}$ represents the average SNR in both S-RIS and RIS-D sub-channels, and N_0 is the noise power spectral density at D.

2.3. PDF of the end-to-end SNR

The PDF of SNR's system, $f_\gamma(\gamma)$, is computed from the SNRs, γ_h, and γ_g. The gain of system is given by $h\mu e^{j\theta} g$, where the quantity $\mu e^{j\theta}$ is deterministic in contrast to h and g. They are random variables. The PDF of SNR's system, $f_\gamma(\gamma)$, is evaluated as [20].

$$f_\gamma(\gamma) = \int_0^\infty f_{\gamma_h}(t) f_{\gamma_g}\left(\frac{\gamma}{t}\right)\frac{1}{t}\, dt \tag{12}$$

where $f_{\gamma_h}(\cdot)$ is the PDFs of the S-RIS, and $f_{\gamma_g}(\cdot)$ is the RIS-D sub-channel's SNRs. Assuming that similar weather conditions over both parts of the channel. A combined distribution, including turbulence levels, pointing errors, and atmospheric attenuation model them. The PDF, $f_{\gamma_i}(\gamma_i)$ is expressed as (13).

$$f_{\gamma_i}(\gamma_i) = \frac{\xi^2}{2(X_l A_0)^{\xi^2}} \frac{\gamma^{(\frac{\xi^2}{2})-1}}{\bar{\gamma}^{\frac{\xi^2}{2}}}\frac{1}{\sqrt{\pi}} e^b \times \mathrm{erfc}\left(\frac{(\frac{1}{2})ln\left[\frac{\gamma_i}{(X_l^2 A_0^2 \bar{\gamma}_i)}\right]+a}{\sqrt{2}\sigma_I}\right) \tag{13}$$

where $i \in \{h, g\}$, $a = 0.5\sigma_I^2 + \sigma_I^2 \xi^2$ and $b = (\sigma_I^2 \xi^2 (1 + \xi^2))/2$. We sequentially substitute γ_i by t and $\frac{\gamma}{t}$ in (13), and obtain $f_{\gamma_h}(t)$ and $f_{\gamma_g}(\frac{\gamma}{t})$ respectively as (14) (15).

$$f_{\gamma_h}(t) = \frac{\xi^2}{2(X_l A_0)^{\xi^2}} \frac{t^{(\frac{\xi^2}{2})-1}}{\bar{\gamma}_h^{\frac{\xi^2}{2}}}\frac{1}{\sqrt{\pi}} e^b \times \mathrm{erfc}\left(\frac{(\frac{1}{2})ln\left[\frac{t}{(X_l^2 A_0^2 \bar{\gamma}_h)}\right]+a}{\sqrt{2}\sigma_I}()\right) \tag{14}$$

$$f_{\gamma_g}\left(\frac{\gamma}{t}\right) = \frac{\xi^2}{2(X_l A_0)^{\xi^2}} \frac{\gamma^{(\frac{\xi^2}{2})-1}}{\bar{\gamma}_g^{\frac{\xi^2}{2}} t^{(\frac{\xi^2}{2})-1}}\frac{1}{\sqrt{\pi}} e^b \times \mathrm{erfc}\left(\frac{(\frac{1}{2})ln\left[\frac{\gamma}{(X_l^2 A_0^2 \bar{\gamma}_g t)}\right]+a}{\sqrt{2}\sigma_I}()\right) \tag{15}$$

In (14) and (15), $\bar{\gamma}_h$ and $\bar{\gamma}_g$ are average values of the SNRs γ_h and γ_g, respectively. We substitute (14) and (15) in to (12), the pdf of SNR, $f_\gamma(\gamma)$, is evaluated as (16).

$$f_\gamma(\gamma) = \frac{\xi^4}{4(X_l A_0)^{\xi^4}} \frac{\gamma^{(\frac{\xi^2}{2})-1}}{(\bar{\gamma}_g \bar{\gamma}_h)^{\frac{\xi^2}{2}}}\frac{1}{\pi} e^{2b} \times \left(\int_0^{\infty\int} \mathrm{erfc}\left(\frac{(\frac{1}{2})ln\left[\frac{t}{(X_l^2 A_0^2 \bar{\gamma}_h)}\right]+a}{\sqrt{2}\sigma_I}\right)\right.$$
$$\left. \times \mathrm{erfc}\left(\frac{(\frac{1}{2})ln\left[\frac{\gamma}{(X_l^2 A_0^2 \bar{\gamma}_g t)}\right]+a}{\sqrt{2}\sigma_I}()\frac{1}{t}\right)\right) \tag{16}$$

With the help of approximate formula, $\mathrm{erfc}(z_1)\mathrm{erfc}(z_2) \approx \exp\{-c_1(z_1 + z_2) - c_2(z_1^2 + z_2^2)\}$, we solve the integral in (16), and obtain the exact unified PDF of end-to-end SNR. The exact unified PDF of end-to-end SNR, $f_\gamma(\gamma)$, as (17):

$$f_\gamma(\gamma) = \frac{\xi^4}{4(X_l A_0)^{\xi^4}} \frac{\gamma^{(\xi^2/2)-1}}{(\bar{\gamma}_g \bar{\gamma}_h)^{\xi^2/2}}\frac{\ln\gamma}{\pi} e^{2b} \times \exp\left\{-c_1\left(\frac{2a+0.5\ln\left[\gamma/(X_l^4 A_0^4 \bar{\gamma}_h \bar{\gamma}_g)\right]}{\sqrt{2}\sigma_I}\right)-\right.$$
$$\left. -c_2\left(\frac{4a^2+\ln\left[\gamma/(X_l^4 A_0^4 \bar{\gamma}_h \bar{\gamma}_g)\right](1+2a)}{2\sigma_I^2} - 2\frac{2a+0.5\ln\left[\gamma/(X_l^4 A_0^4 \bar{\gamma}_h \bar{\gamma}_g)\right]}{\sqrt{2}\sigma_I}\right)\right\} \tag{17}$$

where $c_1 = 1.095008$, $c_2 = 0.756511$.

3. AVERAGE SYMBOL ERROR RATE CALCULATION

The ASER of FSO systems applying SC-QAM is generally presented as (18) [18].

$$P_{se} = \int_0^{+\infty} P_e(\gamma) f_\gamma(\gamma) d\gamma \tag{18}$$

where $P_e(\gamma)$ is the conditional error probability (CEP). The CEP is described as (19).

$$P_e(\gamma) = 1 - [1 - 2q(M_I)Q(A_I)\sqrt{\gamma}][1 - 2q(M_Q)Q(A_Q\sqrt{\gamma})] \tag{19}$$

In which $A_I = \sqrt{6/((M_I^2 - 1) + r^2(M_Q^2 - 1))}$, $A_Q = \sqrt{6r^2/((M_I^2 - 1) + r^2(M_Q^2 - 1))}$, $q(x) = 1 - 1/x$, $Q(x) = 0.5\,erfc(x/\sqrt{2}), r = d_Q/d_I$.

We assume that SISO sub-channel turbulence processes are independent, uncorrelated, identically distributed, PDF $f_\gamma(\gamma)$ can be decreased to a product of the first-order PDF of each element. The (17) and formula contact between probability density function, the PDF of end-to-end SNR, $f_\gamma(\gamma)$, in the case of weak turbulence channels can be given as (20).

$$\bar{P}_{se}(\gamma) = 2\int_0^\infty q(M_Q)Q(A_Q\sqrt{\gamma})f(\gamma)d\gamma + 2\int_0^\infty q(M_I)Q(A_I\sqrt{\gamma})f(\gamma)d\gamma - 4\int_0^\infty q(M_Q)Q(A_Q\sqrt{\gamma})q(M_I)Q(A_I\sqrt{\gamma})f(\gamma)d\gamma \tag{20}$$

4. NUMERICAL RESULTS AND DISSCUSSION

From (17) and (20), we show numerical outcomes for ASER analysis of the RIS-aided FSO systems. We consider a RIS-assisted FSO link over turbulence channel in which S and D are situated at the same distance, $L = 1500$ m, from the RIS as shown in Figure 1. The two system's sub-channels are characterized by the same Index of refraction structure, C_n^2. Parameters and constants considered in our analysis are presented in Table 1.

First, we analyze the average symbol error rate, ASER versus transmitter beam waist radius ω_0 for various values of pointing error displacement standard deviation, σ_s. The system's ASER is described as a function of the transmitter beam waist radius under several pointing error displacement standard deviations. Figure 2 shows that with a given condition that includes specific values of the number of relay stations, aperture radius, and average SNR, the minimum of ASER could be reached to a particular transmitter beam waist radius value ($\omega_0 \approx 0.022\,m$).

Table 1. System parameters and constants

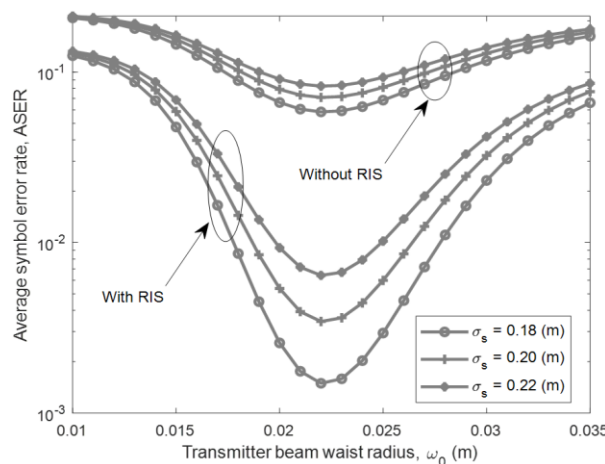| Parameter	Symbol	Value
Laser Wavelength	λ	1,550 nm
Photodetector responsivity	$\Re$	1 A/W
Modulation Index	κ	1
Total noise variance	N_0	10^{-7}A/Hz
Quadrature amplitude modulation	$M_I \times M_Q$	8×4
Receiver aperture diameter	D	$0.06m$
Index of refraction structure	C_n^2	$10^{-15}m^{-2/3}$

Figure 2. ASER performance versus transmitter beam waist radius ω_0 for various values of σ_s

Figure 3 shows the ASER performance against the pointing error displacement standard deviation under several transmitter beam waist radius values. Both RIS and without RIS are considered. The system's ASER is improved significantly with the RIS-aided FSO link. The impact of the RIS-aided and the transmitter beam waist radius on the system's performance is more meaningful in low-pointing error displacement standard deviation regions than in the high areas.
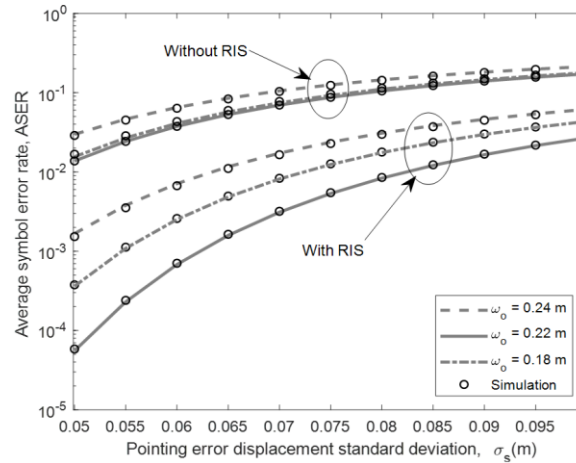

Figure 3. ASER performance against the pointing error displacement standard deviation σ_s for various values of transmitter beam waist radius ω_0

5. CONCLUSION

This study introduced unified and closed-form expressions for the PDF of a RIS-aided FSO link over log-normal atmospheric turbulence and pointing errors. This system's performance was evaluated through ASER. We find terms for ASER performance of ASER systems reckoning with the different transmitter beam waist radius and pointing error displacement standard deviation. The simulation results indicated the influence of RIS-aided on the system's performance, and the ASER falls with RIS-aided. We can see that the simulation outcomes closely conform with the analytical results.

REFERENCES

[1] M. Z. Chowdhury, M. Shahjalal, S. Ahmed, and Y. M. Jang, "6G wireless communication systems: applications, requirements, technologies, challenges, and research directions," *IEEE Open Journal of the Communications Society*, vol. 1, pp. 957–975, 2020, doi: 10.1109/OJCOMS.2020.3010270.

[2] Y. Kaymak, R. Rojas-Cessa, J. Feng, N. Ansari, M. Zhou, and T. Zhang, "A survey on acquisition, tracking, and pointing mechanisms for mobile free-space optical communications," *IEEE Communications Surveys and Tutorials*, vol. 20, no. 2, pp. 1104–1123, 2018, doi: 10.1109/COMST.2018.2804323.

[3] H. A. Duong, V. L. Nguyen, and K. T. Luong, "Misalignment fading effects on the ACC performance of relay-assisted MIMO/FSO systems over atmospheric turbulence channels," *International Journal of Electrical and Computer Engineering (IJECE)*, vol. 12, no. 1, pp. 966–973, Feb. 2022, doi: 10.11591/ijece.v12i1.pp966-973.

[4] K. O. Odeyemi and P. A. Owolawi, "On the performance of energy harvesting AF partial relay selection with TAS and outdated channel state information over identical channels," *International Journal of Electrical and Computer Engineering (IJECE)*, vol. 10, no. 5, pp. 5296–5305, Oct. 2020, doi: 10.11591/ijece.v10i5.pp5296-5305.

[5] D. H. Ai, "Average channel capacity of amplify-and-forward MIMO/FSO systems over atmospheric turbulence channels," *International Journal of Electrical and Computer Engineering (IJECE)*, vol. 8, no. 6, pp. 4334–4342, Dec. 2018, doi: 10.11591/ijece.v8i6.pp4334-4342.

[6] M. Najafi and R. Schober, "Intelligent reflecting surfaces for free space optical communication," in *2019 IEEE Global Communications Conference (GLOBECOM)*, Dec. 2019, pp. 1–7, doi: 10.1109/GLOBECOM38437.2019.9013840.

[7] D. H. Ai and V. L. Nguyen, "BER analysis of amplify-and-forward relaying FSO systems using APD receiver over strong atmospheric turbulence channels," *International Journal of Electrical and Computer Engineering (IJECE)*, vol. 9, no. 5, pp. 3678–3686, Oct. 2019, doi: 10.11591/ijece.v9i5.pp3678-3686.

[8] L. Yang, W. Guo, D. B. da Costa, and M.-S. Alouini, "Free-Space optical communication with reconfigurable intelligent surfaces," *arXiv preprint arXiv: 2012.00547*, Nov. 2020.

[9] H. Wang, Z. Zhang, B. Zhu, J. Dang, and L. Wu, "Two new approaches to optical IRSs: schemes and comparative analysis," *arXiv preprint arXiv: 2012.15398*, Dec. 2020.

[10] A. R. Ndjiongue, T. M. N. Ngatched, O. A. Dobre, and H. Haas, "Design of a power amplifying-RIS for free-space optical communication systems," *arXiv preprint arXiv: 2104.03449*, Apr. 2021.

[11] M. Zeng, X. Li, G. Li, W. Hao, and O. A. Dobre, "Sum rate maximization for IRS-assisted uplink NOMA," *IEEE Communications Letters*, vol. 25, no. 1, pp. 234–238, Jan. 2021, doi: 10.1109/LCOMM.2020.3025978.

[12] M. A. ElMossallamy, H. Zhang, L. Song, K. G. Seddik, Z. Han, and G. Y. Li, "Reconfigurable intelligent surfaces for wireless communications: principles, challenges, and opportunities," *IEEE Transactions on Cognitive Communications and Networking*, vol. 6, no. 3, pp. 990–1002, Sep. 2020, doi: 10.1109/TCCN.2020.2992604.

[13] S. Atapattu, R. Fan, P. Dharmawansa, G. Wang, J. Evans, and T. A. Tsiftsis, "Reconfigurable intelligent surface assisted two-way communications: performance analysis and optimization," *IEEE Transactions on Communications*, vol. 68, no. 10, pp. 6552–6567, Oct. 2020, doi: 10.1109/TCOMM.2020.3008402.

[14] E. Basar, "Reconfigurable intelligent surface-based index modulation: a new beyond MIMO paradigm for 6G," *IEEE Transactions on Communications*, vol. 68, no. 5, pp. 3187–3196, May 2020, doi: 10.1109/TCOMM.2020.2971486.

[15] D. H. Ai, C. D. Vuong, and D. T. Dang, "Average symbol error rate analysis of reconfigurable intelligent surfaces-assisted free-space optical link over log-normal turbulence channels," *International Journal of Electrical and Computer Engineering (IJECE)*, vol. 13, no. 1, pp. 571–578, Feb. 2023, doi: 10.11591/ijece.v13i1.pp571-578.

[16] D. Wang, C. Watkins, and H. Xie, "MEMS mirrors for LiDAR: A review," *Micromachines*, vol. 11, no. 5, Apr. 2020, doi: 10.3390/mi11050456.

[17] C. U. Hail, A.-K. U. Michel, D. Poulikakos, and H. Eghlidi, "Optical metasurfaces: evolving from passive to adaptive," *Advanced Optical Materials*, vol. 7, no. 14, Jul. 2019, doi: 10.1002/adom.201801786.

[18] D. H. Ai, H. D. Trung, and D. T. Tuan, "On the ASER performance of amplify-and-forward relaying MIMO/FSO systems using SC-QAM signals over log-normal and gamma-gamma atmospheric turbulence channels and pointing error impairments," *Journal of Information and Telecommunication*, vol. 4, no. 3, pp. 267–281, Jul. 2020, doi: 10.1080/24751839.2020.1732734.

[19] Z. Yigit, E. Basar, and I. Altunbas, "Low complexity adaptation for reconfigurable intelligent surface-based MIMO systems," *IEEE Communications Letters*, vol. 24, no. 12, pp. 2946–2950, Dec. 2020, doi: 10.1109/LCOMM.2020.3014820.

[20] L. Yang, F. Meng, J. Zhang, M. O. Hasna, and M. Di Renzo, "On the performance of RIS-assisted dual-hop UAV communication systems," *IEEE Transactions on Vehicular Technology*, vol. 69, no. 9, pp. 10385–10390, Sep. 2020, doi: 10.1109/TVT.2020.3004598.

[21] T. Ma, Y. Xiao, X. Lei, P. Yang, X. Lei, and O. A. Dobre, "Large intelligent surface assisted wireless communications with spatial modulation and antenna selection," *IEEE Journal on Selected Areas in Communications*, vol. 38, no. 11, pp. 2562–2574, Nov. 2020, doi: 10.1109/JSAC.2020.3007044.

[22] J. Ye, S. Guo, and M.-S. Alouini, "Joint reflecting and precoding designs for SER minimization in reconfigurable intelligent surfaces assisted MIMO systems," *IEEE Transactions on Wireless Communications*, vol. 19, no. 8, pp. 5561–5574, Aug. 2020, doi: 10.1109/TWC.2020.2994455.

[23] H. Wang *et al.*, "Performance of wireless optical communication with reconfigurable intelligent surfaces and random obstacles," *arXiv preprint arXiv:2001.05715*, Jan. 2020.

[24] L. Yang, F. Meng, Q. Wu, D. B. da Costa, and M.-S. Alouini, "Accurate closed-form approximations to channel distributions of RIS-aided wireless systems," *IEEE Wireless Communications Letters*, vol. 9, no. 11, pp. 1985–1989, Nov. 2020, doi: 10.1109/LWC.2020.3010512.

[25] M. Di Renzo, M. Iezzi, and F. Graziosi, "On diversity order and coding gain of multisource multirelay cooperative wireless networks with binary network coding," *IEEE Transactions on Vehicular Technology*, vol. 62, no. 3, pp. 1138–1157, Mar. 2013, doi: 10.1109/TVT.2012.2229476.

[26] M. Di Renzo, A. Guidotti, and G. E. Corazza, "Average rate of downlink heterogeneous cellular networks over generalized fading channels: a stochastic geometry approach," *IEEE Transactions on Communications*, vol. 61, no. 7, pp. 3050–3071, Jul. 2013, doi: 10.1109/TCOMM.2013.050813.120883.

BIOGRAPHIES OF AUTHORS

Duong Huu Ai 🆔 ⃞ SC ⃝ he received the Master of Electronic Engineering from Danang University of Technology, Vietnam, in 2011, and the Ph.D. degree in Electronics and Telecommunications from Hanoi University of Technology, Vietnam, in 2018. Currently, he is a lecturer at Vietnam-the Korea University of Information and Communication Technology, The University of Danang, Vietnam. His research interests include optical wireless communications, optical and quantum electronics, 5G wireless communications and broadband networks, and IoT. He can be contacted at email: dhai@vku.udn.vn.

Dai Tho Dang 🆔 ⃞ SC ⃝ he received the Master of Computer Sciences from the Nice Sophia Antipolis, France, in 2010, and the Ph.D. degree from Yeungnam University, Republic of Korea, in cooperation with the Wrocław University of Science and Technology, Poland, in 2020. Currently, he works as a lecturer at Vietnam-Korea University of Information and Communication Technology, The University of Danang, Vietnam. His research interests include Statistical Models, Collective Intelligence, and Evolutionary Computation. He can be contacted at email: ddtho@vku.udn.vn.

Nguyen Vu Anh Quang ⓘ 🔗 SC ↻ he received the Master of Electronic Engineering from Danang University of Technology, Vietnam, in 2011, a Ph.D. degree in Electronics and Telecommunications from Soongsil University in 2016. Currently, he is a lecturer at The University of Danang, Vietnam-Korea University of Information and Communication Technology, Danang, Vietnam. His research interests include wireless sensor network, visible light communication, Embedded system. He can be contacted at nvaquang@vku.udn.vn.

Van Loi Nguyen ⓘ 🔗 SC ↻ he received his Master of Engineering in Computer Science from the University of Danang, Vietnam in 2010, a Ph.D. degree from Soongsil University in 2017. Currently, he is a lecturer at The University of Danang, Vietnam-Korea University of Information and Communication Technology, Danang, Vietnam. His research interests include multimedia, information retrieval, artificial intelligence, database, and IoT. He ca be contacted at email: nvloi@vku.udn.vn.